



REPORT

 OPEN ACCESS

## Quantitative characterization of the mechanism of action and impact of a ‘proteolysis-permitting’ anti-PCSK9 antibody

Ryan J. Hansen<sup>a</sup>, Michael J. Berna<sup>a</sup>, Andrea E. Sperry<sup>a</sup>, Thomas P. Beyer <sup>a</sup>, Victor J. Wroblewski <sup>a</sup>, Krista M. Schroeder<sup>a</sup>, and Patrick I. Eacho<sup>b</sup>

<sup>a</sup>Lilly Research Laboratories, Eli Lilly and Company, Indianapolis, IN, USA; <sup>b</sup>Eli Lilly and Company (Ret.)

### ABSTRACT

A recent report described a novel mechanism of action for an anti-proprotein convertase subtilisin-kexin type 9 (PCSK9) monoclonal antibody (LY3015014, or LY), wherein the antibody has improved potency and duration of action due to the PCSK9 epitope for LY binding. Unlike other antibodies, proteolysis of PCSK9 can occur when LY is bound to PCSK9. We hypothesized that this allowance of PCSK9 cleavage potentially improves LY efficiency through two pathways, namely lack of accumulation of intact PCSK9 and reduced clearance of LY. A quantitative modeling approach is necessary to further understand this novel mechanism of action. We developed a mechanism-based model to characterize the relationship between antibody pharmacokinetics, PCSK9 and LDL cholesterol levels in animals, and used the model to better understand the underlying drivers for the improved efficiency of LY. Simulations suggested that the allowance of cleavage of PCSK9 resulting in a lack of accumulation of intact PCSK9 is the major driver of the improved potency and durability of LY. The modeling reveals that this novel ‘proteolysis-permitting’ mechanism of LY is a means by which an efficient antibody can be developed with a total antibody dosing rate that is lower than the target production rate. We expect this engineering approach may be applicable to other targets and that the mathematical models presented herein will be useful in evaluating similar approaches.

**Abbreviations:** PCSK9, proprotein convertase subtilisin-kexin type 9; LY, LY3015014; FL PCSK9, full-length PCSK9; PK, pharmacokinetics; PD, pharmacodynamics; PCSK9 NF, n-terminal fragment of PCSK9 following proteolysis; LDL-C, LDL cholesterol; AMG, an IgG4 antibody with complementarity-determining region sequences of AMG145 anti-PCSK9 antibody; N218, c-terminal fragment of PCSK9 following proteolysis; TMDD, target-mediated drug disposition; AUC, area under the concentration-time curve; IP, immunoprecipitated; MRM, multiple reaction monitoring; WT, wild-type

### ARTICLE HISTORY

Received 18 October 2016  
Revised 29 November 2016  
Accepted 30 November 2016

### KEYWORDS



Antibody; PCSK9;  
pharmacokinetics;  
pharmacodynamics; PKPD;  
proteolysis-permitting

### Introduction

Proprotein convertase subtilisin-kexin type 9 (PCSK9) is an important regulator of serum LDL cholesterol (LDL-C) in animals and humans.<sup>1–4</sup> There is genetic evidence for this role of LDL-C modulation by PCSK9,<sup>1,5–8</sup> as well as impressive clinical pharmacologic evidence for this role, as shown by administration of anti-PCSK9 antibodies. Over the past several years, data from late-stage clinical trials have demonstrated the LDL-C lowering efficacy of several anti-PCSK9 antibodies, such as alirocumab (REGN727/SAR236553, Praluent<sup>®</sup>), evolocumab (AMG145, Repatha<sup>®</sup>) and bococizumab (RN316), and alirocumab and evolocumab were both approved by the US Food and Drug Administration during 2015 for the lowering of LDL-C in some patients.<sup>9,10</sup>

We recently described a PCSK9 antibody with a novel mechanism of action.<sup>11</sup> Unlike other reported catalytic domain PCSK9 inhibitory antibodies, LY3015014 (LY) binds to a PCSK9 epitope that allows cleavage of the intact active form

of PCSK9 to the inactive, 52-kDa form by protease cleavage at Arg218 in the catalytic domain. LY binds N-terminally to the cleavage site, so LY will bind and inhibit full-length (FL) PCSK9 binding to LDL-receptor, but since it allows cleavage of the protein, FL PCSK9 levels do not accumulate in the serum of the animals. Other PCSK9 antibodies caused significant accumulation of FL PCSK9 in humans and animals.<sup>11,12</sup> It was shown that LY allowance of PCSK9 cleavage led to increased potency and durability of effect on LDL-C levels compared with antibodies that did not allow this cleavage. It was also shown that PCSK9-mediated clearance of LY was diminished relative to other anti-PCSK9 antibodies. However, the relative importance of the lack of FL PCSK9 accumulation and the diminished target-mediated clearance of LY was unclear. Additionally, LY maintains the ability to bind to the cleaved 7–8 kDa N-terminal fragment (NF) of PCSK9, and the potential effect of this fragment on the overall efficacy of LY was also unclear.

**CONTACT** Ryan J. Hansen  [hansenry@lilly.com](mailto:hansenry@lilly.com)  Eli Lilly and Company, Lilly Corporate Center, Indianapolis, IN 46285, USA.

Published with license by Taylor & Francis Group, LLC © Eli Lilly & Company

This is an Open Access article distributed under the terms of the Creative Commons Attribution-NonCommercial-NoDerivatives License (<http://creativecommons.org/licenses/by-nc-nd/4.0/>), which permits non-commercial re-use, distribution, and reproduction in any medium, provided the original work is properly cited, and is not altered, transformed, or built upon in any way.

Given the complexity of the pharmacologic system, we hypothesized that mechanism-based pharmacokinetics (PK)/pharmacodynamics (PD) modeling would allow us to gain greater insight into the mechanism of action of LY, including the relative importance of the various contributors of the unexpected potency and long duration of action of LY. Other groups have reported various PK, PK/PD or systems pharmacology models to describe various PCSK9 antibodies.<sup>13-15</sup> However, the unique mechanism of LY has not been explored previously via quantitative models. Here, we present a model-based characterization of the LY-PCSK9 system, and use the model to show that the cleavage of PCSK9 in the presence of LY, leading to a reduction of FL PCSK9 accumulation, is the primary driver of the efficiency of LY. We also show that the residual binding of LY to PCSK9 NF likely has minimal impact on the therapeutic efficiency of LY.

The primary goal of an antibody therapeutic to a soluble ligand is to reduce free ligand levels, thereby diminishing ligand binding to its receptor. Free ligand levels are determined by the ratio of the input rate of the ligand to the clearance of the free ligand. The mechanism for an antibody to reduce free ligand levels following steady-state dosing is the provision of an additional clearance pathway for the free ligand (i.e., the antibody). Thus, if the antibody is cleared along with the ligand, the lowest possible dosing rate of antibody required to neutralize all of the ligand will equal the ligand production rate itself, no matter how high the affinity of the interaction between antibody and ligand.<sup>15,16</sup> This can be problematic in the case of ligands with very high production rates because it limits the feasibility of developing a therapeutic that can practically be administered (e.g., due to solubility and dose volume limitations, and cost).

To lower the absolute dose requirements for a high-production target, antibodies may be developed that allow differential clearance of the antibody and ligand, thus increasing the efficiency of the antibody therapy by allowing more than one ligand molecule to be eliminated by a single antibody binding site. One way to achieve this increased efficiency is to develop an antibody with pH-dependent binding, allowing the antibody to recycle to plasma after endocytosis after releasing the ligand within the cell to be eliminated. This strategy was first reported by Igawa et al.,<sup>16</sup> and was subsequently termed ‘antigen-sweeping’ when applied to antibodies with increased affinity for the FcRn receptor.<sup>17</sup> Chaparro-Riggers et al.<sup>18</sup> subsequently applied this approach to anti-PCSK9 antibodies. In this work, we quantitatively characterize a new possible mechanism for enhancing the therapeutic efficiency of an anti-PCSK9 antibody and for reducing the potential dosing requirements of an antibody to a level lower than the ligand production rate, namely allowing cleavage of the active ligand when bound to the antibody, or a ‘proteolysis-permitting’ antibody.

## Results

### PK/PD modeling of LY effects on PCSK9 levels in mice expressing human wild-type or non-cleavable PCSK9

A mechanism-based PK/PD model was developed to characterize the previously published experiments<sup>11</sup> to facilitate further understanding and investigation of the unique mechanism of action of LY compared with other anti-PCSK9 antibodies. The schematic representation of the final PK/PD model developed to characterize the effects of LY, AMG (an antibody that blocks

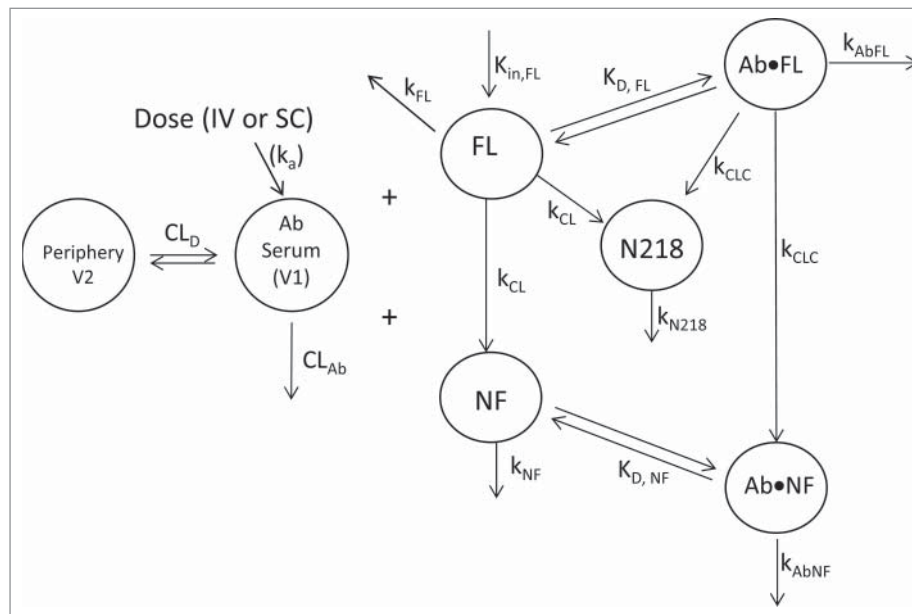


**Figure 1.** Schematic representation of the antibody-ligand portion of the PK/PD model. Antibody (Ab) can be administered either intravenously (IV) or subcutaneously (SC). For SC administration, absorption is governed by a 1st-order rate constant ( $k_a$ ).  $V_1$  represents the volume of distribution of the plasma/serum compartment for Ab. Ab can distribute to a peripheral compartment (with a distribution clearance of  $CL_D$  and a volume for the peripheral compartment of  $V_2$ ). Clearance of Ab from is from the central compartment ( $CL_{Ab}$ ). Binding of Ab to PCSK9 is assumed to be fast relative to other processes and is modeled with an equilibrium constant for binding ( $K_{D,FL}$  for Ab interaction with intact PCSK9, and  $K_{D,NF}$  for interaction with the 7.7 kDa N-terminal fragment following furin cleavage of FL PCSK9). None of the antibodies studied can bind to the C-terminal fragment following furin cleavage (N218), and LY is assumed to bind to FL PCSK9 and PCSK9 NF with equal affinity. Each of the species of PCSK9 has their respective 1st-order rate constants for elimination ( $k_{FL}$ ,  $k_{NF}$  and  $k_{N218}$  for FL PCSK9, PCSK9 NF and N218, respectively). FL PCSK9 is assumed to be produced by a zero-order process ( $k_{in,FL}$ ). Furin cleavage of FL PCSK9 is governed by the 1st-order  $k_{CL}$ . Cleavage of the Ab-bound FL PCSK9 is governed by  $k_{CLC}$ . The Ab-FL PCSK9 complex has a unique 1st-order elimination rate constant  $k_{AbFL}$ , while the Ab-PCSK9 NF complex is assumed to be eliminated by similar processes as free Ab ( $k_{AbNF} = CL_{Ab}/V_1$ ).

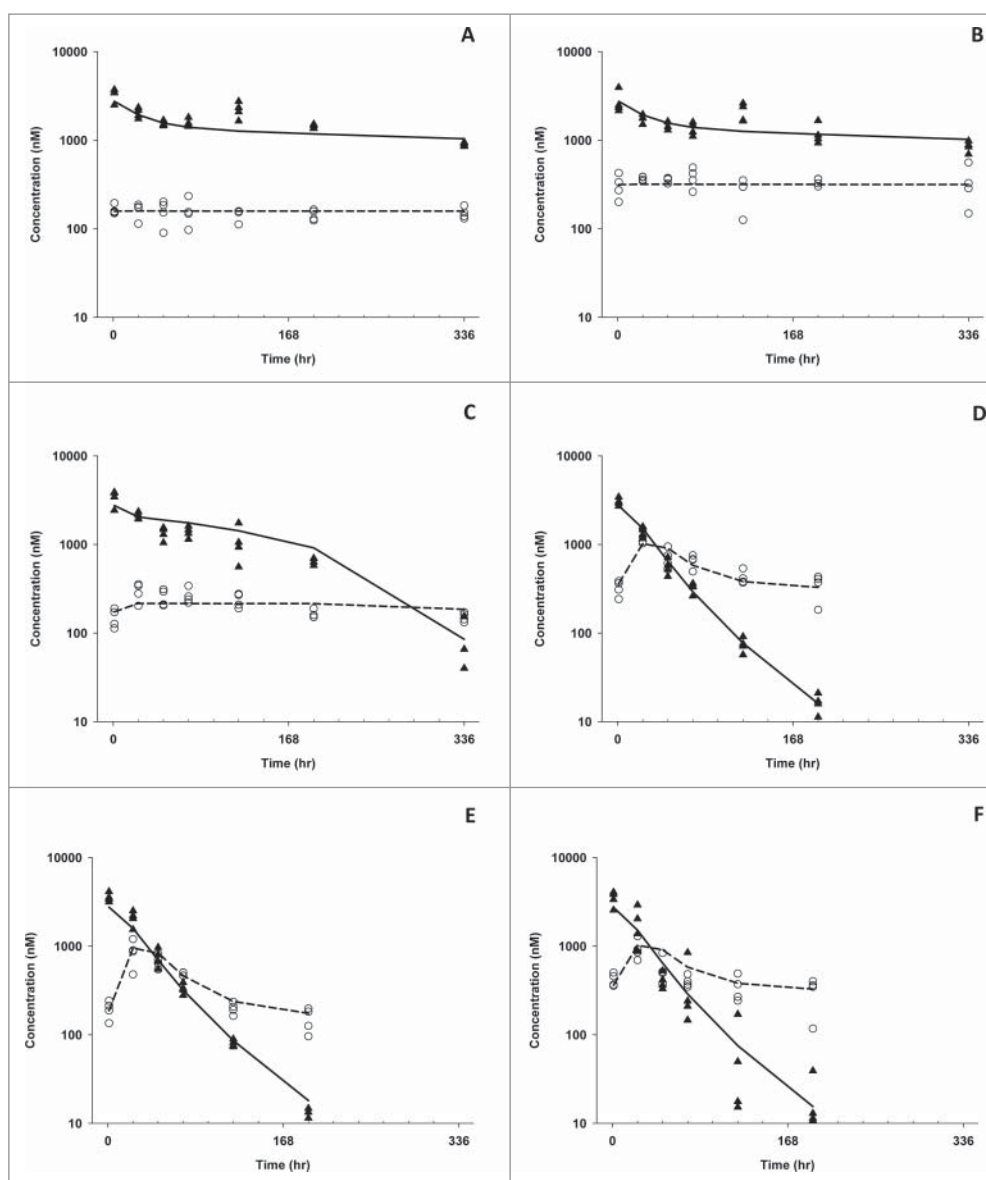


**Figure 2.** Model predicted (lines) and individual observed (symbols) serum IgG concentrations (triangles) and total PCSK9 (FL PCSK9 + N218; circles) following a single 10 mg/kg intravenous dose of control IgG (IgG) to mice expressing wild-type (WT), furin-cleavable PCSK9 (WT-PCSK9, panel A), IgG to mice expressing noncleavable (NC) PCSK9 (NC-PCSK9, panel B), LY to WT-PCSK9 mice (panel C), LY to NC-PCSK9 mice (panel D), AMG to WT-PCSK9 mice (panel E) or AMG to NC-PCSK9 mice (panel F).

PCSK9 proteolysis)<sup>11</sup> and a control IgG on wild-type and non-cleavable PCSK9 is shown in Fig. 1. The system of equations described in the Methods section were used to estimate parameters to predict the antibody and PCSK9 data, and the resulting model predictions vs. raw data plots are shown in Fig. 2, with the selected model and parameterization providing reasonable predictions of the observed data. The parameter estimates from these fits are shown in Table 1.

The mechanism-based nature of the model allows prediction of the suppression of the intact PCSK9, since these levels were not measured in the study. The predicted duration of suppression of FL PCSK9 is significantly longer for LY compared with AMG in mice expressing wild-type PCSK9 (Fig. 3A). However, the predicted duration of suppression of FL PCSK9 in mice expressing non-cleavable PCSK9 was similar (and short) for both antibodies (Fig. 3B). These predictions are consistent with the previously published observations in mice, where LY had a

distinct durability advantage over AMG in its ability to lower LDL-C in mice expressing wild-type human PCSK9 (even though LY has lower affinity for PCSK9 than does AMG), but no such advantage in mice expressing non-cleavable PCSK9.<sup>11</sup>

#### **PK/PD modeling of LY effects on PCSK9 and LDL-C levels in monkeys**

A study was conducted in cynomolgus monkeys that allowed linkage of the predicted suppression of FL PCSK9 to LDL-C in a model that is more representative of humans. The antibody-ligand portion of the model was the same as was developed for mice, with parameter values estimated for monkey. The LDL-C portion of the model was an indirect response PK/PD model,<sup>19</sup> where FL PCSK9 levels inhibit the removal of LDL-C in a concentration-dependent manner. The equation governing the LDL-C portion of the model is also shown in Methods.

**Table 1.** PK/PD model parameters describing the interaction of antibody and PCSK9 for control IgG, LY and AMG in mice expressing wild-type (cleavable) and non-cleavable human PCSK9. Values are mean (SE).

| Parameter   | IgG                 | LY                          | AMG                 |
|---|---------------------|-----------------------------|---------------------|
| $CL_{Ab}$ (mL hr <sup>-1</sup> kg <sup>-1</sup> ) |                     | 0.0786 (0.0219)             |                     |
| $V_1$ (mL kg <sup>-1</sup> )                      |                     | 47.5 (3.13)                 |                     |
| $CL_D$ (mL hr <sup>-1</sup> kg <sup>-1</sup> )    |                     | 0.845 (0.166)               |                     |
| $V_2$ (L kg <sup>-1</sup> )                       |                     | 44.1 (5.31)                 |                     |
| $K_{in}$ (nM hr <sup>-1</sup> )                   |                     | 62.4 (4.67)                 |                     |
| $k_{FL}$ (hr <sup>-1</sup> )                      |                     | 0.198 (0.0150)              |                     |
| $k_{CL}$ (hr <sup>-1</sup> )                      |                     | 0.357 (0.0314) <sup>c</sup> |                     |
| $k_{AbFL}$ (hr <sup>-1</sup> )                    |                     | 0.0447 (0.00424)            |                     |
| $k_{AbNF}$ (hr <sup>-1</sup> )                    |                     | 0.00165 <sup>b</sup>        |                     |
| $k_{NF}$ (hr <sup>-1</sup> )                      |                     | 3.57 <sup>b</sup>           |                     |
| $k_{N218}$ (hr <sup>-1</sup> )                    |                     | 0.893 <sup>b</sup>          |                     |
| $k_{CLC}$ (hr <sup>-1</sup> )                     | 0 <sup>a</sup>      | 0.357(0.0314) <sup>c</sup>  | 0 <sup>a</sup>      |
| $K_{D,FL}$ (nM)                                   | 100000 <sup>a</sup> | 2.00 <sup>a</sup>           | 0.310 <sup>a</sup>  |
| $K_{D,NF}$ (nM)                                   | 100000 <sup>a</sup> | 2.00 <sup>a</sup>           | 100000 <sup>a</sup> |

<sup>a</sup>Fixed:  $K_{D,FL}$  and  $K_{D,NF}$  for IgG and  $K_{D,NF}$  for AMG fixed at arbitrarily high value, as the binding of these species is negligible.  $K_{D,FL}$  for LY and AMG, and  $K_{D,FL}$  for AMG were fixed to in vitro values.  $k_{CLC}$  is assumed to be zero for AMG as AMG inhibits cleavage of PCSK9;  $k_{CLC}$  was also set to zero for IgG.

<sup>b</sup>Derived:  $k_{AbNF} = CL_{Ab}/V_1$ ;  $k_{NF} = 10k_{CL}$ ;  $k_{N218} = 2.5k_{CL}$

<sup>c</sup> $k_{CL}$  and  $k_{CLC} = 0$  for all antibodies in the animals expressing non-cleavable PCSK9.

Model-predicted versus observed data for the PK of LY are shown in Fig. 4 (intravenous dose results shown in panel A and subcutaneous dose results shown in panel B). The model predictions captured the non-linearity in the PK, caused by target-mediated drug disposition (TMDD), quite well. The observed vs. predicted total (FL PCSK9 + N218) PCSK9 concentrations are shown in Fig. 5A. Total PCSK9 levels remained near baseline following dosing of LY to cynomolgus monkeys, whereas they increased dramatically when an antibody that prevents PCSK9 cleavage was dosed (Fig. 5B). Fig. 6 shows the observed vs. model predicted LDL-C levels, showing the model was successfully able to link the predicted suppression of free intact PCSK9 to the suppression of LDL-C in monkeys. The PK and PD parameters associated with this model are shown in Table 2.

### Simulations to understand the importance of improved antibody clearance vs improved FL PCSK9 elimination and reduction of FL PCSK9 accumulation

We hypothesized that the benefits of the LY mechanism of action may be through either reduced accumulation of the FL PCSK9 or through reduced TMDD of the anti-PCSK9

antibody.<sup>11</sup> We conducted simulations to probe the effect of reducing TMDD for antibodies that bind to PCSK9. Fig. 7A shows the effect of reducing TMDD for an antibody that binds PCSK9 but prevents cleavage of the PCSK9 (an AMG-like antibody). In this case, reducing TMDD actually decreases the effectiveness of the antibody for lowering FL PCSK9 levels. Fig. 7B shows the effect of decreasing non-target mediated clearance on antibody effectiveness. We generated a hypothetical antibody like LY, but added an additional, non-target clearance pathway for this antibody to give it a PK profile similar to an antibody like AMG. This additional non-target mediated clearance pathway led to diminished FL PCSK9 lowering compared with LY, suggesting that improving non-target mediated clearance has the potential to improve antibody effectiveness. However, this hypothetical LY-like antibody with faster clearance still had better FL PCSK9 lowering efficacy than an antibody like AMG, showing that clearance is not fully responsible for the improved effects of LY. Taken together, these observations suggest that the improved clearance of LY is an effect of the unique mechanism of action and is not the cause of the increased efficiency of LY. By simply improving the target-mediated clearance alone, without adding the elimination pathway for antibody-bound FL PCSK9 (thus reducing the accumulation of FL PCSK9), one would not necessarily expect improved efficiency for the anti-PCSK9 antibody.

### Simulations to understand the importance of PCSK9 NF binding to LY

Since LY is able to bind PCSK9 NF when PCSK9 is cleaved, we investigated whether this binding would have a significant effect on LY's efficacy for FL PCSK9 lowering. We simulated a version of LY that had insignificant binding to PCSK9 NF and compared the predicted FL PCSK9 lowering to that of LY. As can be seen in Fig. 8, the binding of LY to PCSK9 NF should have very little effect on LY's efficiency of FL PCSK9 lowering.

### Simulations to evaluate the degree of absolute dose reduction possible with the 'proteolysis-permitting' antibodies

The major significance of LY's mechanism of action is that this permission of proteolysis of the active ligand when bound to the anti-ligand antibody can afford a pathway to

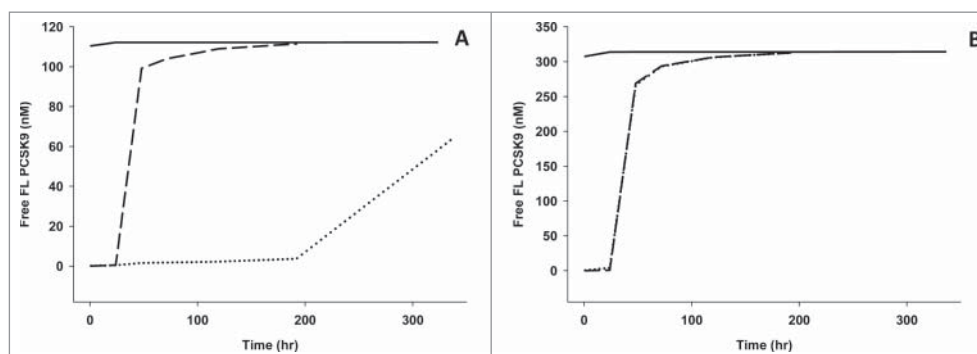


**Figure 3.** Model predicted decreases in free full-length (FL) PCSK9 following 10 mg/kg intravenous doses of IgG (solid black line), LY (dotted line) or AMG (long dash line) to mice expressing WT human PCSK9 (panel A) or NC-PCSK9 (panel B). In NC-PCSK9 mice, the LY and AMG lines overlay.

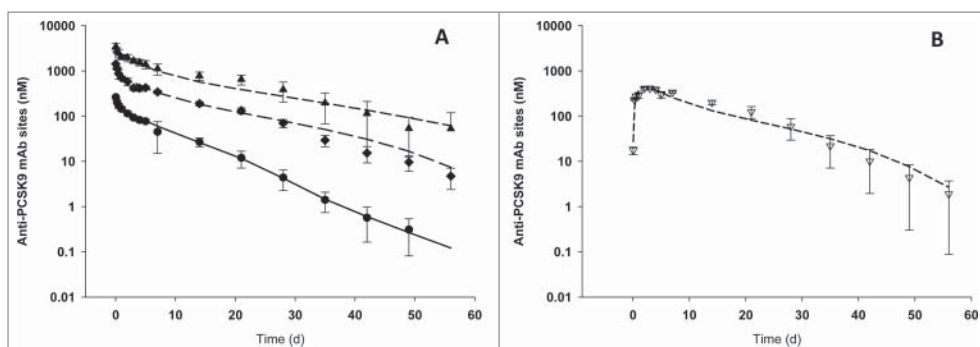


**Figure 4.** PK of LY following IV dosing (panel A) of 1 mg/kg (circles), 5 mg/kg (diamonds) or 15 mg/kg (triangles) LY; or SC dosing (panel B) of 5 mg/kg LY to cynomolgus monkeys. Observed data are represented as mean and SD ( $n = 3-4$ /group) and model predictions are represented with the lines.

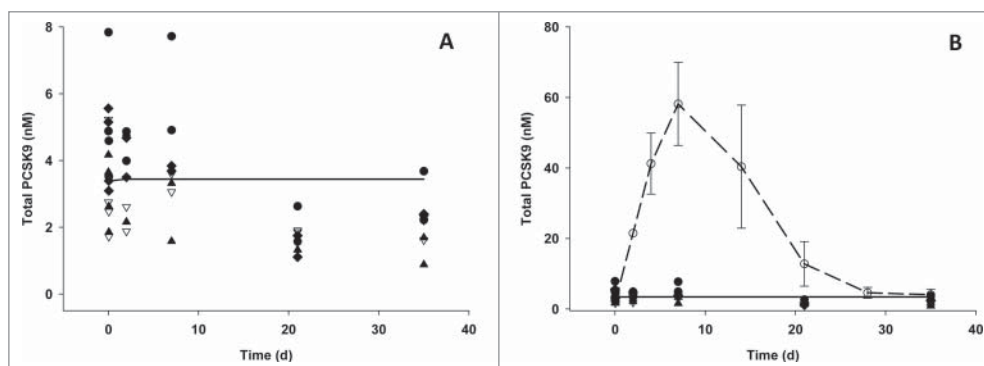


**Figure 5.** Total PCSK9 levels (FL PCSK9 + N218) following IV dosing (panel A) of 1 mg/kg (circles), 5 mg/kg (diamonds) or 15 mg/kg (triangles) LY; or SC dosing of 5 mg/kg LY (inverted open triangles) to cynomolgus monkeys. Individual animal observed data are represented with symbols and model predictions are represented with the black lines. LY is not predicted to increase total PCSK9 levels at any dose level administered. For comparison, panel B shows the same data from panel A, plotted with the total PCSK9 levels (open circles, dashed line; mean and SD) for an antibody (5 mg/kg IV dose) that does not allow cleavage of PCSK9.

lower the absolute dosing requirements of the antibody to less than the input rate of the ligand (and still reach complete inhibition of the ligand). It generates a differential clearance between the ligand and the antibody. To our

knowledge, thus far, only one other approach to increase an antibody's efficiency below the ligand production rate has been described (the pH-dependent release of the ligand, or 'antigen-sweeping' antibody).<sup>16</sup>

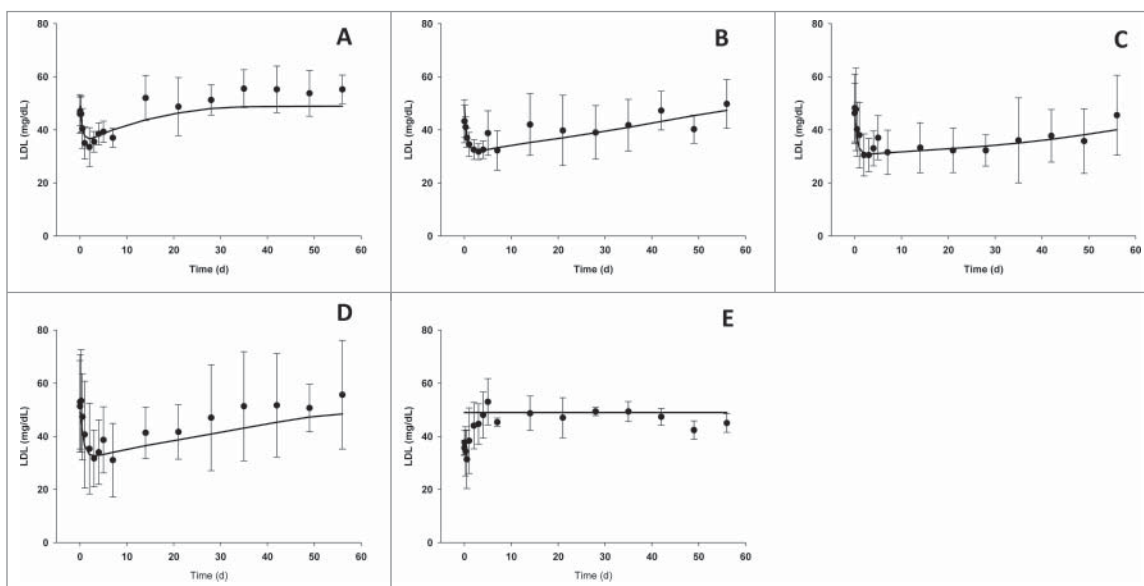


**Figure 6.** Cyno LDL-C following IV dosing of 1 mg/kg (Panel A), 5 mg/kg (Panel B) or 15 mg/kg (Panel C) LY; or SC dosing of 5 mg/kg LY (Panel D) or IV dosing of Control IgG (Panel E) to cynomolgus monkeys. Observed data are represented as mean and SD ( $n = 3-4$ /group) and model predictions are represented with the lines.

**Table 2.** PK/PD model parameters describing the interaction of LY with PCSK9 and the corresponding effects on LDL-C in cynomolgus monkeys.

| Parameter  | Value (SE)           | Parameter   | Value (SE)      |
|--|----------------------|---|-----------------|
| $k_a$ ( $\text{hr}^{-1}$ )                       | 0.0434 (0.00708)     | $K_{in,LDL}$ ( $\text{mg dL}^{-1} \text{hr}^{-1}$ ) | 2.64 (0.518)    |
| F (%)  | 69.7 (7.65)          | $k_{out,LDL}$ ( $\text{hr}^{-1}$ )                  | 0.0872 (0.0172) |
| $CL_{Ab}$ ( $\text{mL hr}^{-1} \text{kg}^{-1}$ ) | 0.283 (0.0288)       | $I_{max}$   | 0.390 (0.0330)  |
| $V_1$ ( $\text{mL kg}^{-1}$ )                    | 71.0 (3.33)          | $IC_{50}$ (nM)                                      | 0.0510 (0.0246) |
| $CL_D$ ( $\text{mL hr}^{-1} \text{kg}^{-1}$ )    | 0.279 (0.0534)       | $\eta_{Kin,LDL}^c$                                  | 0.0281 (0.0101) |
| $V_2$ ( $\text{L kg}^{-1}$ )                     | 55.8 (7.34)          |   |                 |
| $K_{in}$ ( $\text{nM hr}^{-1}$ )                 | 0.511 (0.120)        |   |                 |
| $k_{FL}$ ( $\text{hr}^{-1}$ )                    | 0.0472 (0.0362)      |   |                 |
| $k_{CL}$ ( $\text{hr}^{-1}$ )                    | 0.164 (0.0532)       |   |                 |
| $k_{CLC}$ ( $\text{hr}^{-1}$ )                   | 0.164 (0.0532)       |   |                 |
| $k_{AbFL}$ ( $\text{hr}^{-1}$ )                  | 0.0432 (0.00696)     |   |                 |
| $k_{AbNF}$ ( $\text{hr}^{-1}$ )                  | 0.00399 <sup>b</sup> |   |                 |
| $k_{NF}$ ( $\text{hr}^{-1}$ )                    | 1.64 <sup>b</sup>    |   |                 |
| $k_{N218}$ ( $\text{hr}^{-1}$ )                  | 0.41 <sup>b</sup>    |   |                 |
| $K_{D,FL}$ (nM)                                  | 2.00 <sup>a</sup>    |   |                 |
| $K_{D,NF}$ (nM)                                  | 2.00 <sup>a</sup>    |   |                 |

<sup>a</sup>Fixed:  $K_{D,FL}$  and  $K_{D,NF}$  for LY were fixed to in vitro value.<sup>11</sup>

<sup>b</sup>Derived:  $k_{AbNF} = CL_{Ab}/V_1$ ;  $k_{NF} = 10k_{CL}$ ;  $k_{N218} = 2.5k_{CL}$

<sup>c</sup> $\eta_{Kin,LDL}$  is an inter-animal variability parameter on LDL-C production rate.

Fig. 9 shows simulated dose-response curves for an antibody that allows cleavage of PCSK9 (Fig. 9A) vs. an antibody that prevents cleavage of PCSK9 (Fig. 9B), over a range of affinities for both antibodies. Other than the affinity (and the prevention of cleavage in Fig. 9B), the parameters for these simulations were the same as for LY. These simulations show that increasing affinity of the antibody will lower the dosing requirements to achieve a certain level of PCSK9 lowering, but only to a certain point. Beyond a certain affinity, no additional improvement is seen for either type of antibody. At the limit, for the most optimized antibody and dosing regimen, the lowest input rate for an antibody that prevents ligand proteolysis should equal the ligand production rate. The input rate for PCSK9 in this monkey model is  $0.511 \text{ nM hr}^{-1}$ , with a volume of distribution of  $71.0 \text{ mL kg}^{-1}$  (Table 2). This leads to a weekly PCSK9 production rate of  $6.1 \text{ nmol/kg/week}$ . The model assumes two binding sites per antibody, so the lowest possible input rate to neutralize all PCSK9 for the optimal non-cleaving antibody (perfect  $K_D$ , non-target clearance and antibody input rate) would be  $\sim 0.46 \text{ mg/kg/week}$ . Because LY allows antibody-bound FL

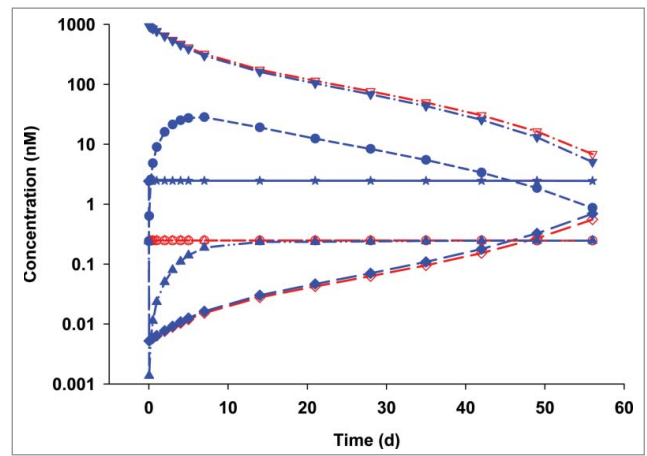


**Figure 8.** Simulations probing the effect of reduced PCSK9 NF binding on the efficiency of LY. LY is shown in blue solid symbols. LY with no PCSK9 NF binding is shown in red open symbols. Total antibody levels are indicated by inverted triangles; total PCSK9 NF levels are circles; free PCSK9 NF levels are stars; free FL PCSK9 levels are diamonds. Antibody dosing was a single IV 5 mg/kg dose.

PCSK9 (AbFL) an additional clearance pathway,  $k_{CLC}$ , the lowest possible dose for the optimal proteolysis-permitting PCSK9 antibody will be  $k_{AbFL}/(k_{AbFL}+k_{CLC})$  times the lowest dose for the antibody that does not allow proteolysis. In this case, that ratio is 0.208, so the optimal proteolysis-permitting antibody can allow doses  $\sim 5$ -fold lower than the PCSK9 production rate and still reach full FL PCSK9 suppression ( $\sim 0.096 \text{ mg/kg/week}$  for antibody dosing). Since neither LY nor our hypothetical LY version that prevents cleavage in Fig. 9 are perfectly idealized with regard to affinity, non-TMDD clearance and dosing rate, the observed doses for full neutralization are slightly higher than these theoretical amounts, but the difference between the two can be clearly seen.

## Discussion

We used data from two animal models to develop and explore the quantitative PK/PD model for the effects of a proteolysis-permitting antibody on circulating PCSK9 and

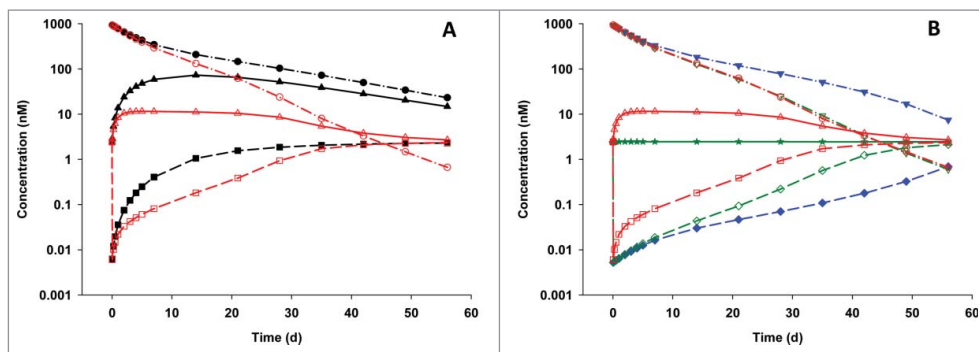


**Figure 7.** Simulations probing the effect of reduced clearance on the efficiency of LY. Panel A shows the effect of eliminating TMDD on FL PCSK9 lowering for an antibody that prevents cleavage of PCSK9 while bound to the antibody. If TMDD is eliminated (closed black symbols), the total antibody PK profile is improved (closed black circles for no TMDD vs open red circles for TMDD), but total FL PCSK9 levels increase (triangles) and free FL PCSK9 levels (squares) are not suppressed as much as the case where TMDD is present. Panel B shows LY (closed symbols, blue) compared with an antibody that prevents cleavage, and still has TMDD (open red circles, triangles and squares for total antibody, total FL PCSK9 and free FL PCSK9, respectively). An antibody that allows cleavage, but has the same PK profile as the antibody that does not allow clearance (by adding a non-ligand dependent clearance route) is shown in open green symbols (inverted triangle for PK, stars for total FL PCSK9 and diamonds for free FL PCSK9). Dosing was single 5 mg/kg IV dose for each antibody scenario.

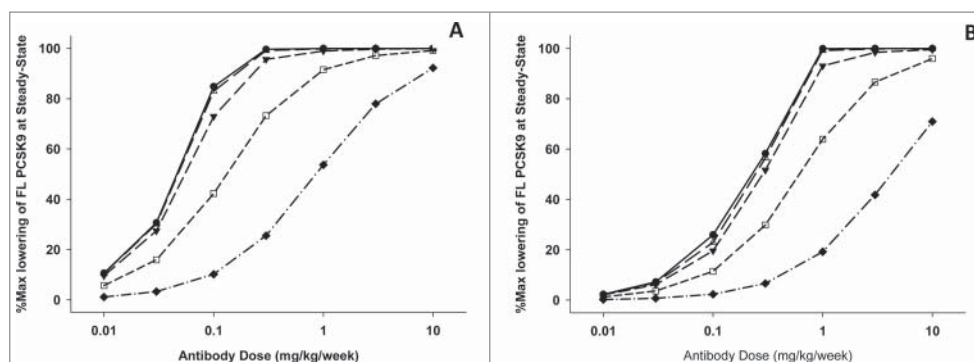


**Figure 9.** Simulations illustrating the maximal dose efficiency for antibodies like LY that allow cleavage (Panel A) compared with an antibody with all LY PK properties, except that it prevents cleavage of the PCSK9 (Panel B). Curves represent predicted fraction of maximum steady-state lowering of FL PCSK9 following 7 weekly doses of antibodies of increasing affinity for PCSK9. Symbols designate antibodies with affinities of 0.02 nM (circles), 0.2 nM (triangles), 2 nM (inverted triangles), 20 nM (squares) and 200 nM (diamonds).

the subsequent effects on LDL-C lowering. Because non-human primates are more similar to humans with respect to PK, PD and LDL-C aspects of the system, this was the primary model with which we wanted to explore the mechanism of action of LY. However, since we had total PCSK9 measurements available (rather than free PCSK9), and because LY does not cause changes to total PCSK9 in primates, the cynomolgus monkey was not the ideal system to develop the structural PK/PD model. Thus, we used the LY and AMG data from the previously published experiments in mice expressing either wild-type human PCSK9 or non-cleavable PCSK9<sup>11</sup> to ensure that the model structure was appropriate to characterize the various antibody-ligand interactions. We then applied that structural model to the more appropriate cynomolgus monkey model for our simulations.

The structural model developed in mice was able to adequately describe the PK and PCSK9 concentrations following dosing of AMG, LY or control IgG to mice expressing either wild-type human PCSK9 or non-cleavable human PCSK9. This model translated directly to the cynomolgus monkey. The mechanism-based model allowed good characterization of both the LY levels and the PCSK9 levels. Further, the pharmacologic utility of the model was demonstrated by linking the predicted FL PCSK9 lowering in monkey to the LDL-C lowering. The model projections matched the observed data very nicely, and demonstrated the ability to link PK, target engagement and downstream biomarker effects. This connectivity of mouse to monkey, and of monkey target levels to monkey LDL-C levels, gave us confidence that the structural model was sufficiently reasonable to further explore various aspects of the mechanism of action of LY.

Few attempts have been made to describe PK/PD modeling incorporating equilibrium binding for two proteins that compete for binding with one receptor (e.g., PCSK9 NF competes with FL PCSK9 for binding to LY). This type of system has previously presented challenges to implement easily in standard PK/PD software, as the solution for the free species involves a cubic equation, and there has been uncertainty regarding which of the three solutions of the cubic equation are permissible. Because of this uncertainty, Yan et al. used a numerical bisection algorithm and a differential representation of the system to describe exogenous IgG competing with endogenous IgG for

binding to FcRn and recombinant human erythropoietin competing with endogenous erythropoietin for binding to the erythropoietin receptor.<sup>20</sup> In our implementation, we used Wang's exact mathematical expression for describing competitive binding of two ligands for a protein molecule, which showed that only one of the solutions to the cubic equation is permissible.<sup>21</sup> This allowed us to avoid the use of the numerical bisection algorithm or the differential representation, and explicitly solve the equations for free antibody, AbFL and AbNF, and readily implement the system of equations shown in the Methods in NONMEM.

We conducted simulations to better understand the importance of improved clearance of LY vs an antibody like AMG to the overall mechanism of action. To do this, we first simulated the expected monkey PCSK9 and antibody profiles for an antibody that prevents cleavage, that does allow target-mediated clearance, and that has the same affinity for FL PCSK9 as LY. Then we conducted an analogous simulation, removing the target-mediated clearance, and assuming the AbFL complex is eliminated like the free antibody. This removal of TMDD for the antibody resulted in an improved PK profile (increased AUC), but actually predicted a worse free FL PCSK9 profile compared with the antibody that allowed TMDD (Fig. 7A). The antibody without TMDD allows the total PCSK9 levels to accumulate even higher than the antibody with TMDD, and the higher total FL PCSK9 levels more than offset the improvements in PK observed.

Another way to try to get at the clearance question was to add a non-ligand dependent antibody clearance pathway to the LY parameters, to generate an antibody with an LY-like proteolysis property, but with additional non-target mediated antibody clearance. This generated a proteolysis-permitting antibody with a PK profile similar to what would be expected of a non-cleaving antibody like AMG. Simulations showed that increasing the LY clearance so that the PK profile matched an antibody like AMG did have a detrimental effect on the FL PCSK9 lowering, compared with LY (Fig. 7B). However, the FL PCSK9 suppression for this faster clearance version of LY was still superior to the suppression for a non-cleaving antibody like AMG. This suggests that improving non-target mediated clearance (LY with fast CL vs. LY) for an antibody can provide better FL PCSK9 lowering. Taken together, these observations

show that the improvement in antibody clearance is not the primary driver of the increased efficiency of an antibody like LY. Rather, the primary driver is the ability of the antibody to allow clearance of the active PCSK9 without clearing the antibody itself. The improved clearance of the antibody that is associated with this mechanism is an inseparably-linked benefit. Thus, to generate antibodies with similar benefits as LY, a strategy that drives a *differential* clearance between the antibody and the ligand, not simply improving the clearance of the antibody, should be used.

Glassman and Balthasar recently reported a physiologically based PK model that nicely characterized the effect of pH-dependent binding antibodies on reducing the target-mediated clearance of anti-PCSK9 antibodies, showing quantitatively the impact of that mechanism on the improvement of antibody PK.<sup>15</sup> In that analysis, they did not report the influence of the mechanism of action on the ligand levels themselves, but we would expect that the key driver for the improved efficiency of this class of antibodies is the differential clearance generated between antibody and ligand, and not solely the improved antibody clearance or minimization of TMDD. In developing efficient antibodies for high ligand production targets, it is important to focus on strategies that drive differential clearance of the antibody and the ligand, and not solely on improving antibody clearance. One could conceivably eliminate TMDD and improve the antibody PK by mechanisms other than pH-dependent binding or allowance of ligand proteolysis. For example, two approaches might be to inhibit the interaction between PCSK9 and APLP2,<sup>11,22</sup> or to simply lower the affinity of the antibody-PCSK9 interaction; however, we would predict that the dosing benefits observed for LY and pH-dependent antibodies would not be present in such cases if there is no improvement in the differential clearance of the antibody and the ligand.

On the surface, it would seem that the ability of LY to bind to the inactive PCSK9 NF might decrease the efficacy of LY therapy, since it competes for binding sites with FL PCSK9. However, since the affinity for PCSK9 NF and FL PCSK9 are equivalent, and the binding is always assumed to be in equilibrium, the fractional binding of each fragment will be identical. Once full-length, antibody-bound PCSK9 is cleaved, total FL PCSK9 levels decrease, and the equilibrium between LY, FL PCSK9 and PCSK9 NF is immediately re-established, and the PCSK9 NF binding has little effect on FL PCSK9 lowering. In this way, LY effectively provides an additional clearance pathway for FL PCSK9, and allows differential clearance between antibody and ligand.

In summary, we developed a quantitative model to characterize the mechanism of action of a novel, efficient, 'proteolysis-permitting' antibody. This is a second demonstrated mechanism of action that has the potential to reduce the total dosing requirements to a level below the input rate of the ligand. For the LY mechanism and target, the potential reduction in dosing rate relative to antigen production rate, and relative to antibodies that do not allow proteolysis of PCSK9, is ~5-fold. Finding ways to improve efficiency of antibody therapy can be critical to success for antibodies to ligands with high production rates. We emphasize that the strategy for improving antibody therapy efficiency should

include more than reducing antibody clearance or increasing antibody affinity. One should also consider ways to provide differential clearance between the antibody and the ligand. Mechanism-based mathematical models such as the model herein described can be extremely helpful in providing insight into antibody-ligand systems, as they can provide insight into target kinetics and suppression. Consideration of variables such as the nature of the target, its production and elimination kinetics, its elimination mechanisms, the epitope of binding relative to proteolysis, activity of cleaved fragments, and feasibility of introducing pH-dependent binding between antibody and ligand should inform engineering strategies for antibodies directed against soluble targets.

## Materials and methods

### Materials

The anti-PCSK9 and IgG4 control antibodies used in the studies were described elsewhere.<sup>11</sup> Each are provided by Eli Lilly and Company. LY is an IgG4 anti-PCSK9 antibody that binds to the catalytic domain of PCSK9 and allows proteolytic cleavage when bound. AMG is an IgG4 antibody with complementarity-determining region sequences of AMG145 anti-PCSK9 antibody. H2a6 is another Lilly-generated anti-PCSK9 IgG4 antibody that prevents proteolysis of PCSK9 when bound.

### Mouse PK/PD study

The mouse PK/PD study was described in detail elsewhere.<sup>11</sup> Briefly, mice expressing either wild-type human PCSK9 or the non-cleavable (R215A/R218A) PCSK9 mutant were dosed with a single intravenous dose of 10 mg/kg control IgG4 (IgG), AMG or LY (n = 12–16 mice per group). Serum was collected for up to 2 weeks post-dose and analyzed for total human IgG levels and total PCSK9 levels (the sum of antibody-bound and free FL PCSK9 and N218).

### Monkey PK/PD study

Normal chow-fed cynomolgus monkeys were randomized by LDL-C levels and received a single intravenous (1, 5 or 15 mg/kg) or subcutaneous (5 mg/kg) dose of LY or a single intravenous dose (5 mg/kg) of control hIgG4. Blood samples for PK, PCSK9 and LDL-C levels were collected for up to 56 d post-dose. LDL-C levels were determined with a homogeneous assay (LDL-C plus second generation; Roche Diagnostics) using a Roche P800 Modular Analytics analyzer.

For comparison, PCSK9 results from a second monkey study are also shown. In this study an antibody preventing the proteolysis of PCSK9 (antibody H2a6) was dosed intravenously to monkeys at 5 mg/kg.

All animal protocols were approved by the Eli Lilly and Company Animal Care and Use Committee.

### IA-LC/MS/MS assay to measure human IgG in mouse serum

LY, AMG, or IgG concentrations were measured in mouse serum by high resolution/accurate mass (HR/AM) LC/MS



following immunoaffinity sample preparation. A stable isotope-labeled antibody was added to the samples as an internal standard, and the human IgGs were immunoprecipitated (IP) from serum aliquots through the addition of goat anti-human IgG-biotin (Southern Biotech, cat# 2049-08) and streptavidin-coated magnetic beads (DynaMyl M280, cat# 112.06D). Following IP, the complex-associated magnetic beads were washed with phosphate-buffered saline, and the IgGs were eluted with formic acid. The eluents were concentrated to dryness, and the samples were reduced (triethylphosphine), alkylated (2-iodoethanol); and digested overnight with trypsin (Promega Gold, cat# V5280). Aliquots (20  $\mu$ L) were injected onto the LC/MS for analysis. The assay was qualified to quantify human IgG concentrations in mouse serum over the range of 100 to 12,800 ng/mL.

The LC/MS analyses were performed on a Thermo Orbitrap Elite mass spectrometer operated in the positive ion electrospray, full scan FTMS mode. A surrogate peptide from the hinge region of the IgG was selected for accurate mass precursor quantification, while surrogate peptides from the Fab region and C-terminus of the heavy chain were measured to ensure analyte selectivity and in vivo stability. The liquid chromatography system used a Thermo Acela UHPLC liquid chromatograph and a HTS Pal Leap autosampler. Chromatographic separation was on an Analytical Sales Sprite Armor C18 column (2.1 $\times$ 80 mm, 5  $\mu$ m), which were operated at 40 C. The mobile phases (0.1% formic acid in either water (MP A) or acetonitrile [MP B]) were delivered at 0.4 mL/min using a linear gradient (min/% MP B): 0.0/5, 1.0/5, 7.0/40, 7.1/5, 8.0/5.

### Immunoassay to measure LY in monkey serum

Concentrations of LY were determined using a sandwich ELISA method for human IgG, using goat anti-human  $\kappa$  IgG (Southern Biotech, cat# 2060-01) and horseradish peroxidase-conjugated mouse anti-human Fc IgG (Southern Biotech, cat# 9040-05) for capture and detection, respectively. The curve range was 5 to 400 ng/mL with a lower and upper limit of quantitation of 10 and 300 ng/mL, respectively (Advion Biosciences).

### IA-LC/MS/MS assay to measure PCSK9 in monkey and mouse serum

Total PCSK9 concentrations in cynomolgus monkey or mouse serum were analyzed by LC/MS/MS following 'drug-tolerant' immunoaffinity-capture sample preparation. Serum aliquots were added to an Immulon 4 HBX ELISA plate (ThermoFisher Scientific) that was coated with a drug-tolerant PCSK9 monoclonal antibody (Eli Lilly) and blocked. Following incubation at ambient temperature, the plate was washed and PCSK9 was eluted from the ELISA plate using acidic acetonitrile containing 40 ng/mL of SIL PCSK9 surrogate peptide internal standard (DVI<sub>7</sub>NEAWFPEDQR). The eluents were concentrated to dryness, and the samples were digested overnight with trypsin. Aliquots (20  $\mu$ L) were injected onto the LC/MS/MS for analysis. The assay was qualified to quantify PCSK9 concentrations in monkey and mouse serum over the range of 31.2 (monkey PCSK9 and

non-cleavable human PCSK9 in mouse) or 62.5 (wild-type human PCSK9 in mouse) to 1000 ng/mL.

The LC/MS/MS analyses were performed on a Thermo Quantum triple quadrupole mass spectrometer operated in the positive ion electrospray, multiple reaction monitoring (MRM) mode. The following MRM transitions were monitored for PCSK9 (DVINEAWFPEDQR surrogate tryptic peptide): 809.9  $\rightarrow$  644.1 (CE 25 eV, tube lens 113 V), and for the SIL internal standard (DVI<sub>7</sub>NEAWFPEDQR synthetic peptide): 813.4  $\rightarrow$  644.1 (CE 25 eV, tube lens 120 V). The liquid chromatography system used a Thermo Acela UHPLC liquid chromatograph and a HTS Pal Leap autosampler. Chromatographic separation was on an Analytical Sales Sprite Armor C18 column (2.1 $\times$ 40 mm, 4  $\mu$ m) with a Thermo Javelin Aquasil C18 (2.1 $\times$ 20 mm, 5  $\mu$ m) guard column, which were operated at 50 C. The mobile phases (0.1% formic acid in water (MP A) or acetonitrile [MP B]) were delivered at 0.5 mL/min using a linear gradient (min/% MP B): 0.0/5, 0.5/5, 3.25/35, 3.26/5, 3.5/5.

### Mathematical model to characterize interaction between anti-PCSK9 antibodies, PCSK9 and LDL-C

#### IgG-PCSK9 portion of model

The structural PK/PD model to characterize the interaction between anti-PCSK9 antibodies and PCSK9 levels was generated in mice expressing either wild-type (WT), cleavable human PCSK9 or non-cleavable-PCSK9. Then, the structural model developed in mice was applied directly to monkeys. Thus, the antibody-ligand binding portion of the model was the same between the two species and was described by the system of equations below:

$$\begin{aligned} \frac{dAb_{sc}}{dt} &= -k_a \times Ab_{sc} \\ \frac{dAb_t}{dt} &= \frac{k_a \times Ab_{sc}}{V_1} - k_{Ab} \times Ab_f - k_{12} \times Ab_f - k_{AbFL} \times AbFL \\ &\quad - k_{AbNF} \times AbNF + \frac{k_{21} \times Ab_p}{V_1} \end{aligned}$$

$$\frac{dAb_p}{dt} = k_{12} \times Ab_f \times V_1 - k_{21} \times Ab_p$$

$$\begin{aligned} \frac{dFL_t}{dt} &= K_{in} - k_{FL} \times FL_f - k_{CL} \times FL_f - k_{AbFL} \times AbFL \\ &\quad - k_{CLC} \times AbFL \end{aligned}$$

$$\begin{aligned} \frac{dNF_t}{dt} &= k_{CL} \times FL_f + k_{CLC} \times AbFL - k_{NF} \times NF_f \\ &\quad - k_{AbNF} \times AbNF \end{aligned}$$

$$\frac{dN218_t}{dt} = k_{CL} \times FL_f + k_{CLC} \times AbFL - k_{N218} \times N218_t$$

Antibody-PCSK9 binding is always assumed to be at equilibrium in this model. LY can bind equally to both PCSK9 NF and FL PCSK9, whereas AMG can bind only to FL PCSK9. Wang described an exact mathematical expression for describing competitive binding of two ligands to a protein.<sup>21</sup> Based on that solution, the following equations

can be developed:

$$Ab_f = -\frac{a}{3} + \frac{2}{3}\sqrt{(a^2 - 3b)} \times \cos\left(\frac{\theta}{3}\right)$$

$$Ab_{FL} = \frac{FL_t(2\sqrt{(a^2 - 3b)} \times \cos(\frac{\theta}{3}) - a)}{3K_{D,FL} + (2\sqrt{(a^2 - 3b)} \times \cos(\frac{\theta}{3}) - a)}$$

$$Ab_{NF} = \frac{NF_t(2\sqrt{(a^2 - 3b)} \times \cos(\frac{\theta}{3}) - a)}{3K_{D,NF} + (2\sqrt{(a^2 - 3b)} \times \cos(\frac{\theta}{3}) - a)}$$

where

$$a = K_{D,FL} + K_{D,NF} + FL_t + NF_t - Ab_t$$

$$b = K_{D,NF}(FL_t - Ab_t) + K_{D,FL}(NF_t - Ab_t) + K_{D,FL} \times K_{D,NF}$$

$$c = -K_{D,FL} \times K_{D,NF} \times Ab_t$$

$$\theta = \arccos\left(\frac{-2a^3 + 9ab - 27c}{2\sqrt{(a^2 - 3b)^3}}\right)$$

Once  $Ab_f$ ,  $Ab_{FL}$  and  $Ab_{NF}$  have been obtained, the remaining species can be obtained using mass balance equations:

$$FL_f = FL_t - Ab_{FL}$$

$$NF_f = NF_t - Ab_{NF}$$

In these equations the various species of antibody, ligand and antibody-ligand complexes are defined as follows:  $Ab_{sc}$  is the mass of antibody at the subcutaneous site (monkey only);  $Ab_t$  is the concentration of total antibody binding sites in the central (plasma/serum) compartment ( $Ab_t = Ab_f + Ab_{FL} + Ab_{NF}$ );  $Ab_f$  is the concentration of free antibody binding sites in the central compartment;  $Ab_{FL}$  is the concentration of antibody-intact full length PCSK9 (FL PCSK9) conjugate;  $Ab_{NF}$  is the concentration of antibody-N-terminally truncated PCSK9 fragment (PCSK9 NF) conjugate;  $Ab_p$  is the mass of antibody in the peripheral distribution compartment;  $FL_t$  is the concentration of total full-length, intact PCSK9 ( $FL_f + Ab_{FL}$ );  $FL_f$  is the free full-length, intact PCSK9;  $NF_t$  is the concentration of total N-terminally truncated PCSK9 fragment ( $NF_f + Ab_{NF}$ );  $NF_f$  is the concentration of free N-terminal fragment;  $N218_t$  is the concentration of total C-terminal PCSK9 fragment following furin cleavage of PCSK9 ( $N218_t = N218_f$  since neither of the antibodies bind to N218).

In these equations the various rate constants are defined as follows:  $k_a$  is a rate constant for antibody absorption;  $k_{Ab}$  is a rate constant for free antibody elimination (parameterized as the ratio of antibody clearance to central compartment volume of distribution -  $CL_{Ab}/V_1$ );  $k_{12}$  and  $k_{21}$  are rate constants governing antibody distribution to and from the peripheral compartment (parameterized as the ratios of antibody distributional clearance to volume of distribution -  $k_{12} = CL_D/V_1$  and  $k_{21} = CL_D/V_2$ );  $k_{Ab_{FL}}$  is a rate constant governing elimination of  $Ab_{FL}$ ;  $k_{Ab_{NF}}$  is a rate constant governing elimination of  $Ab_{NF}$  (for these analyses it was assumed  $k_{Ab_{NF}} = k_{Ab}$ );  $K_{in}$  is the production rate constant for intact PCSK9;  $k_{FL}$  is the rate

constant for elimination of free, intact PCSK9;  $k_{CL}$  is the rate constant for cleavage of free PCSK9 (presumably by furin);  $k_{CLC}$  is the rate constant for cleavage of antibody bound FL PCSK9 ( $k_{CLC} = k_{CL}$  for LY in monkeys and mice expressing WT PCSK9 and  $k_{CLC} = 0$  for AMG in all species and for LY in mice expressing NC PCSK9);  $k_{NF}$  and  $k_{N218}$  are the elimination rate constants for free PCSK9 NF and free N218, respectively.  $K_{D,FL}$  and  $K_{D,NF}$  are the affinities of the antibodies for FL PCSK9 and PCSK9 NF, and were fixed at in vitro values (for non-binding situations, e.g., AMG with PCSK9 NF, these values were fixed at an arbitrarily high value of 1 mM to allow use of the same equations for all antibodies).

The initial conditions for the ligand equations are defined by the following equations (where the 0 subscript represents the concentration of the entity at time zero):

$$FL_0 = \frac{K_{in}}{k_{CL} + k_{FL}}$$

$$NF_0 = \frac{k_{CL}}{k_{NF}} FL_0$$

$$N218_0 = \frac{k_{CL}}{k_{N218}} FL_0$$

The bioanalytical assays provided the measures of  $Ab_t$  and the total PCSK9 (sum of  $FL_t$  and  $N218_t$ ). The above equations allowed the prediction of all other antibody, ligand and antibody-ligand species in the model system.

NONMEM VII was used for estimation to obtain parameter estimates for both mouse and monkey, and for simulation to explore various aspects of the system. All parameters in the model were estimated, with the following exceptions:  $K_D$  values for LY and AMG were fit to in vitro values;<sup>11</sup>  $k_{Ab_{NF}}$  was assumed to be equal to  $k_{Ab}$ ;  $k_{NF}$  and  $K_{N218}$  cannot be reliably estimated from the current data since PCSK9 NF and N218 were not specifically measured. These parameters were fixed such that baseline N218 concentrations would be approximately 30% of total circulating PCSK9 (FL PCSK9+N218) and that baseline PCSK9 NF concentrations would be approximately 10% of circulating FL PCSK9 concentrations. These approximations are consistent with the data regarding the circulating forms of PCSK9 reported previously by Han et al.<sup>23</sup>

#### LDL-C portion of model

For the monkey study, the LDL-C portion of the model was included with the PK and PCSK9 portions of the model to develop the linkage between FL PCSK9 suppression and LDL-C lowering. A basic indirect response model, with FL PCSK9 suppressing the elimination of LDL-C was used for this portion of the model, as denoted below.

$$\frac{dLDL - C}{dt} = K_{in,LDL} - k_{out,LDL} \times \left(1 - \frac{I_{max} \times FL}{IC_{50} + FL}\right) \times LDL - C$$

In this equation,  $K_{in,LDL}$  is a constant production rate for LDL-C;  $k_{out,LDL}$  is a rate constant for elimination of LDL;  $I_{max}$  is the maximum possible inhibition of  $k_{out,LDL}$  by FL PCSK9;  $IC_{50}$  is the FL PCSK9 concentration at which  $k_{out,LDL}$  is 50%

inhibited. All the data (PK, PD and LDL) were used simultaneously to obtain PK/PD parameter estimates in monkey.

### Simulations to explore unique mechanism of action of LY

#### Relative importance of reducing TMDD vs lowering FL PCSK9 accumulation

The PK/PD model and parameters obtained from the monkey estimation were then adapted for use in simulations to explore the unique mechanism of action of LY. First, we generated simulations to explore the relative importance of the decreased clearance that LY's mechanism provides vs. the additional clearance of PCSK9 (and decreased accumulation) that LY's mechanism provides. To investigate the improved antibody clearance on LY's efficacy, we first compared the effects of an antibody that prevents cleavage and has TMDD with an antibody that prevents cleavage and does not have TMDD. We next generated a simulation where we added an additional clearance route for LY to give it the same PK profile it would have if there were no cleavage of the LY-FL PCSK9 complex (while still allowing cleavage of the complex). These two sets of simulations allowed us to consider the effect of improving LY clearance by minimizing TMDD or by improving non-TMDD clearance. We simulated the expected free FL PCSK9 reduction under each of these conditions. See Table 3 for a summary of the parameters used for these simulations.

**Table 3.** PK/PD model parameters for simulations investigating the effects of clearance, accumulation and PCSK9 NF binding.

| Parameter  | <sup>a</sup> LY Yes<br>CLC Yes<br>TMDD | <sup>b</sup> No CLC<br>Yes<br>TMDD | <sup>c</sup> No CLC<br>No TMDD | <sup>d</sup> LY + Fast CL                  | <sup>e</sup> Poor<br>PCSK9 NF<br>affinity |
|--|--|------------------------------------|--------------------------------|--|---|
| CL <sub>Ab</sub> (mL hr <sup>-1</sup> kg <sup>-1</sup> ) | 0.283                                  | 0.283                              | 0.283                          | 0.283                                      | 0.283                                     |
| V <sub>1</sub> (mL kg <sup>-1</sup> )                    | 71.0                                   | 71.0                               | 71.0                           | 71.0                                       | 71.0                                      |
| CL <sub>D</sub> (mL hr <sup>-1</sup> kg <sup>-1</sup> )  | 0.279                                  | 0.279                              | 0.279                          | 0.279                                      | 0.279                                     |
| V <sub>2</sub> (L kg <sup>-1</sup> )                     | 55.8                                   | 55.8                               | 55.8                           | 55.8                                       | 55.8                                      |
| K <sub>in</sub> (nM hr <sup>-1</sup> )                   | 0.511                                  | 0.511                              | 0.511                          | 0.511                                      | 0.511                                     |
| k <sub>FL</sub> (hr <sup>-1</sup> )                      | 0.0472                                 | 0.0472                             | 0.0472                         | 0.0472                                     | 0.0472                                    |
| k <sub>CL</sub> (hr <sup>-1</sup> )                      | 0.164                                  | 0.164                              | 0.164                          | 0.164                                      | 0.164                                     |
| k <sub>CLC</sub> (hr <sup>-1</sup> )                     | 0.164                                  | 0                                  | 0                              | 0.164                                      | 0.164                                     |
| k <sub>AbFL</sub> (hr <sup>-1</sup> )                    | 0.0432                                 | 0.0432                             | 0.00399                        | 0.0432                                     | 0.0432                                    |
| k <sub>AbNF</sub> (hr <sup>-1</sup> )                    | 0.00399                                | 0.00399                            | 0.00399                        | <sup>f</sup> 0.00399 + k <sub>elAb,2</sub> | 0.00399                                   |
| k <sub>NF</sub> (hr <sup>-1</sup> )                      | 1.64                                   | 1.64                               | 1.64                           | 1.64                                       | 1.64                                      |
| k <sub>N218</sub> (hr <sup>-1</sup> )                    | 0.41                                   | 0.41                               | 0.41                           | 0.41                                       | 0.41                                      |
| K <sub>D,FL</sub> (nM)                                   | 2.00                                   | 2.00                               | 2.00                           | 2.00                                       | 2.00                                      |
| K <sub>D,NF</sub> (nM)                                   | 2.00                                   | 1000000                            | 1000000                        | 2.00                                       | 1000000                                   |
| V <sub>max</sub> (nM hr <sup>-1</sup> )                  | NA                                     | NA                                 | NA                             | <sup>g</sup> 0.450                         | NA  |
| K <sub>m</sub> (nM)                                      | NA                                     | NA                                 | NA                             | <sup>g</sup> 37.0                          | NA  |

<sup>a</sup>LY column values are the parameters obtained for LY in the monkey study (Table 2).

<sup>b</sup>No CLC Yes TMDD column indicates an AMG-like antibody that prevents cleavage and has TMDD (Fig 7A,7B).

<sup>c</sup>No CLC No TMDD column indicates an antibody that prevents cleavage and prevents TMDD (Fig 7A).

<sup>d</sup>LY + Fast CL column indicates an antibody like LY with an additional non-PCSK9 mediated clearance added to obtain a PK profile similar to the No CLC Yes TMDD antibody (Fig 7B).

<sup>e</sup>Poor PCSK9 NF affinity column indicates an antibody that allows cleavage like LY and has poor binding to PCSK9 NF (Fig 8).

<sup>f</sup>k<sub>AbNF</sub> is equal to the antibody elimination rate constant (k<sub>Ab</sub> = CL<sub>Ab</sub>/V<sub>1</sub>). For LY + Fast CL, the antibody has an additional, non-linear elimination pathway so it will match the PK profile for No CLC Yes TMDD. In this case k<sub>AbNF</sub> is the sum of the original antibody elimination rate constant and the secondary elimination pathway, k<sub>elAb,2</sub>.

<sup>g</sup>k<sub>elAb,2</sub> is a non-linear secondary elimination pathway (non-PCSK9 mediated clearance). k<sub>elAb,2</sub> = V<sub>max</sub>/(K<sub>m</sub> + C<sub>Ab</sub>).

### Impact of residual PCSK9 NF binding to LY

Because LY binds equally to PCSK9 NF and FL PCSK9, we were interested to explore the effect of this PCSK9 NF binding on the efficiency of FL PCSK9 lowering by LY. We generated simulations where K<sub>D,NF</sub> for LY was set to an arbitrarily high value (1 mM) and compared the lowering of FL PCSK9 under these parameter conditions with those of the base case (using the actual monkey parameters). Table 3 shows the parameter values used in this simulation.

### Impact of LY mechanism of action on lowest absolute dose

We explored the effect of LY's mechanism of action, and its ability to lower the absolute dose for an optimal therapeutic antibody. To find the 'optimal' antibody, we generated a series of simulations wherein we made a set of antibodies with LY's mechanism of action, but with a range of affinities for PCSK9 (both FL PCSK9 and PCSK9 NF) varying from 20 pM to 200 nM. We simulated weekly dosing (7 weeks) over a dose range of 0.01–10 mg/kg and calculated area under the curve (AUC) of FL PCSK9 at steady-state. We repeated these simulations for an antibody that prevents cleavage, and compared minimum dosing requirements for an antibody like LY that allows cleavage to an inactive form, and an antibody that does not allow cleavage. The lowering of FL PCSK9 at steady-state was expressed as the % of maximum inhibition, with maximum inhibition being defined as the baseline FL PCSK9 levels multiplied by the dosing interval of 168 hr.

### Disclosure of potential conflicts of interest

Each author is, or has been, an employee and/or shareholder of Eli Lilly and Company.

### Acknowledgments

The authors thank Julian Davies, Barrett Allan, and Ryan Darling for engineering LY; Hana Baker, Cindy Shrake, Courtney Wooden, Charles Reidy, Patrick Forler, and Aaron Austin for their work on the studies in mice; and Bing Han for helpful discussions and suggestions.

### ORCID

Thomas P. Beyer  <http://orcid.org/0000-0002-6374-9700>

Victor J. Wroblewski  <http://orcid.org/0000-0002-0593-4350>

### References

- Abifadel M, Varret M, Rabes JP, Allard D, Ouguerram K, Devillers M, Cruaud C, Benjannet S, Wickham L, Erlich D, et al. Mutations in PCSK9 cause autosomal dominant hypercholesterolemia. *Nat Genet* 2003; 34:154–6; PMID:12730697; <http://dx.doi.org/10.1038/ng1161>
- Maxwell KN, Breslow JL. Adenoviral-mediated expression of Pcsk9 in mice results in a low-density lipoprotein receptor knockout phenotype. *Proc Natl Acad Sci U S A* 2004; 101:7100–5; PMID:15118091; <http://dx.doi.org/10.1073/pnas.0402133101>
- Rashid S, Curtis DE, Garuti R, Anderson NN, Bashmakov Y, Ho YK, Hammer RE, Moon YA, Horton JD. Decreased plasma cholesterol and hypersensitivity to statins in mice lacking Pcsk9. *Proc Natl Acad Sci U S A* 2005; 102:5374–9; PMID:15805190; <http://dx.doi.org/10.1073/pnas.0501652102>

4. Horton JD, Cohen JC, Hobbs HH. PCSK9: a convertase that coordinates LDL catabolism. *J Lipid Res* 2009; 50 Suppl:S172-7; PMID:19020338; <http://dx.doi.org/10.1194/jlr.R800091-JLR200>
5. Cunningham D, Danley DE, Geoghegan KF, Griffor MC, Hawkins JL, Subashi TA, Varghese AH, Ammirati MJ, Culp JS, Hoth LR, et al. Structural and biophysical studies of PCSK9 and its mutants linked to familial hypercholesterolemia. *Nat Struct Mol Biol* 2007; 14:413-9; PMID:17435765; <http://dx.doi.org/10.1038/nsmb1235>
6. Cohen J, Pertsemlidis A, Kotowski IK, Graham R, Garcia CK, Hobbs HH. Low LDL cholesterol in individuals of African descent resulting from frequent nonsense mutations in PCSK9. *Nat Genet* 2005; 37:161-5; PMID:15654334; <http://dx.doi.org/10.1038/ng1509>
7. Cohen JC, Boerwinkle E, Mosley TH, Jr, Hobbs HH. Sequence variations in PCSK9, low LDL, and protection against coronary heart disease. *N Engl J Med* 2006; 354:1264-72; PMID:16554528; <http://dx.doi.org/10.1056/NEJMoa054013>
8. Kotowski IK, Pertsemlidis A, Luke A, Cooper RS, Vega GL, Cohen JC, Hobbs HH. A spectrum of PCSK9 alleles contributes to plasma levels of low-density lipoprotein cholesterol. *Am J Hum Genet* 2006; 78:410-22; PMID:16465619; <http://dx.doi.org/10.1086/500615>
9. Bergeron N, Phan BA, Ding Y, Fong A, Krauss RM. Proprotein convertase subtilisin/kexin type 9 inhibition: a new therapeutic mechanism for reducing cardiovascular disease risk. *Circulation* 2015; 132:1648-66; PMID:26503748; <http://dx.doi.org/10.1161/CIRCULATIONAHA.115.016080>
10. Latimer J, Batty JA, Neely DD, Kunadian V. PCSK9 inhibitors in the prevention of cardiovascular disease. *J Thromb Thrombolysis* 2016; 42(3):405-19; PMID:27095708; <http://dx.doi.org/10.1007/s11239-016-1364-1>
11. Schroeder KM, Beyer TP, Hansen RJ, Han B, Pickard RT, Wroblewski VJ, Kowala MC, Eacho PI. Proteolytic Cleavage of Antigen Extends the Durability of an Anti-PCSK9 Monoclonal Antibody. *J Lipid Res* 2015; 56(11):2124-32; PMID:26392590; <http://dx.doi.org/10.1194/jlr.M061903>
12. Roth EM, McKenney JM, Hanotin C, Asset G, Stein EA. Atorvastatin with or without an antibody to PCSK9 in primary hypercholesterolemia. *N Engl J Med* 2012; 367:1891-900; PMID:23113833; <http://dx.doi.org/10.1056/NEJMoa1201832>
13. Budha NR, Leabman M, Jin JY, Wada DR, Baruch A, Peng K, Tingley WG, Davis JD. Modeling and Simulation to Support Phase 2 Dose Selection for RG7652, a Fully Human Monoclonal Antibody Against Proprotein Convertase Subtilisin/Kexin Type 9. *AAPS J* 2015; 17:881-90; PMID:25823668; <http://dx.doi.org/10.1208/s12248-015-9750-8>
14. Gadkar K, Budha N, Baruch A, Davis JD, Fielder P, Ramanujan S. A Mechanistic Systems Pharmacology Model for Prediction of LDL Cholesterol Lowering by PCSK9 Antagonism in Human Dyslipidemic Populations. *CPT Pharmacometrics Syst Pharmacol* 2014; 3:e149; PMID:25426564; <http://dx.doi.org/10.1038/psp.2014.47>
15. Glassman PM, Balthasar JP. Application of a catenary PBPK model to predict the disposition of "catch and release" anti-PCSK9 antibodies. *Int J Pharm* 2016; 505:69-78; PMID:27041125; <http://dx.doi.org/10.1016/j.ijpharm.2016.03.066>
16. Igawa T, Ishii S, Tachibana T, Maeda A, Higuchi Y, Shimaoka S, Moriyama C, Watanabe T, Takubo R, Doi Y, et al. Antibody recycling by engineered pH-dependent antigen binding improves the duration of antigen neutralization. *Nat Biotechnol* 2010; 28:1203-7; PMID:20953198; <http://dx.doi.org/10.1038/nbt.1691>
17. Igawa T, Maeda A, Haraya K, Tachibana T, Iwayanagi Y, Mimoto F, Higuchi Y, Ishii S, Tamba S, Hironiwa N, et al. Engineered monoclonal antibody with novel antigen-sweeping activity in vivo. *PLoS One* 2013; 8:e63236; PMID:23667591; <http://dx.doi.org/10.1371/journal.pone.0063236>
18. Chaparro-Riggers J, Liang H, DeVay RM, Bai L, Sutton JE, Chen W, Geng T, Lindquist K, Casas MG, Boustany LM, et al. Increasing serum half-life and extending cholesterol lowering in vivo by engineering antibody with pH-sensitive binding to PCSK9. *J Biol Chem* 2012; 287:11090-7; PMID:22294692; <http://dx.doi.org/10.1074/jbc.M111.319764>
19. Dayneka NL, Garg V, Jusko WJ. Comparison of four basic models of indirect pharmacodynamic responses. *J Pharmacokinet Biopharm* 1993; 21:457-78; PMID:8133465; <http://dx.doi.org/10.1007/BF01061691>
20. Yan X, Chen Y, Krzyzanski W. Methods of solving rapid binding target-mediated drug disposition model for two drugs competing for the same receptor. *J Pharmacokinet Pharmacodyn* 2012; 39:543-60; PMID:22926955; <http://dx.doi.org/10.1007/s10928-012-9267-z>
21. Wang ZX. An exact mathematical expression for describing competitive binding of two different ligands to a protein molecule. *FEBS Lett* 1995; 360:111-4; PMID:7875313; [http://dx.doi.org/10.1016/0014-5793\(95\)00062-E](http://dx.doi.org/10.1016/0014-5793(95)00062-E)
22. DeVay RM, Shelton DL, Liang H. Characterization of Proprotein Convertase Subtilisin/Kexin Type 9 (PCSK9) Trafficking Reveals a Novel Lysosomal Targeting Mechanism via Amyloid Precursor-like Protein 2 (APLP2). *J Biol Chem* 2013; 288:10805-18; PMID:23430252; <http://dx.doi.org/10.1074/jbc.M113.453373>
23. Han B, Eacho PI, Knierman MD, Troutt JS, Konrad RJ, Yu X, Schroeder KM. Isolation and characterization of the circulating truncated form of PCSK9. *J Lipid Res* 2014; 55:1505-14; PMID:24776539; <http://dx.doi.org/10.1194/jlr.M049346>